

Electric Vehicle Battery Pack Design for Mitigating Thermal Runaway Propagation

Ewan Copsey

Department of Engineering,
Durham University
Durham, UK
ewan.d.copsey@durham.ac.uk

Hongjian Sun

Department of Engineering,
Durham University
Durham, UK
hongjian.sun@durham.ac.uk

Jing Jiang

Department of Mathematics, Physics &
Electrical Engineering, Northumbria University
Newcastle, UK
jing.jiang@northumbria.ac.uk

Abstract—The production of electric vehicle battery packs with ever-increasing energy densities has accelerated the electrification of the world’s automotive industry. With increased attention on the electric vehicle markets, it is vital to increase the safety of these vehicles which now hold higher hazardous potential. This paper aims to explore the field of pack-level thermal runaway mechanisms and evaluate potential mitigation strategies. Most available literature concentrates on the micromanagement of thermal runaway whereas this paper takes a more holistic approach. Thermal simulations for analysing thermal runaway of modules in differing locations are run to characterise the behaviour of a thermal runaway event at pack-level. Results suggest that the propagation of thermal runaway is consistently severe in a cooling plate cooled battery pack as the cooling plate acts as a channel for high temperatures. Additionally, thermal insulation added to contain the rapid increase in temperature unfortunately results in wider spread higher temperatures.

Index Terms—Electric Vehicle, Battery Pack Design, Propagation Simulations, Thermal Runaway

I. INTRODUCTION

THE significant growth in the use of electric vehicles (EVs) [1] reflects the world’s desire to move toward a more sustainable future. For example, £1.3 billion is being invested by the UK government to accelerate the roll-out of charge points for electric vehicles [2]. This rapid rise is due to the unprecedented pace of development of more energy-dense batteries. Therefore, there is an ever-greater demand for increasing the energy density of battery packs. However, larger amounts of energy contained in the same space drastically escalates the hazardous potential of battery pack failure.

Thermal runaway occurs when a cell, or area within a cell, achieves elevated temperatures. There are mainly three abuse cases that can lead to thermal runaway, i.e., mechanical abuse, electrical abuse and thermal abuse [3]. Mechanical abuse is defined as the destructive deformation and/or displacement caused by an applied force - most commonly as a result of collisions and penetration. Deformation of the battery pack is commonplace in road accidents which can result in dangerous conditions that trigger more severe hazards: 1) the battery separator becomes damaged and an internal short circuit (ISC) occurs; 2) the flammable electrolyte leaks and potentially

leads to a subsequent fire. ISC is widely cited as the most common cause for thermal runaway [4], [5]. Electrical abuse can be separated into the mismanagement of the battery’s health and external short-circuiting [6]. Thermal abuse is a local overheating that isn’t caused by a previous mechanical or electrical abuse scenario that is almost exclusively caused by a loose contact on the cell connector. These connectors can become loose over time due to vehicle vibration experienced during driving [7], [8]. Thermal runaway propagation events are a major concern for both manufacturers and governments due to the damage caused by the event and the economic impact of losing consumer confidence in the new technology.

If a thermal runaway event is caught in its early stages, prevention mechanisms can be triggered, and the damage caused minimised. Utilising the battery management system’s (BMS) ability to monitor the voltage, current, and temperature is vital in the early detection of an ISC-induced thermal runaway event [6]. Detection of battery ISC is not an industry standard and many different approaches are currently being evaluated in research. Xia *et al.* in [9] presented a fault detection method based on the correlation coefficient of voltage curves. It can detect the initial stage of short circuits by capturing an off-trend voltage drop and relates the variation to the drop in the correlation coefficient of the voltage curves. Contrastingly, Feng *et al.* in [10] successfully used an estimation algorithm coupled with a 3D electrochemical-thermal ISC coupled model to track parameter variations in real-time, thereby making it feasible to detect an instantaneously triggered ISC.

Physical measures can be implemented in the pack design to reduce the likelihood of thermal runaway propagation. Shui *et al.* in [11] noted that the manufacturers need to start considering the design of the pack from a mechanical standpoint as well as higher energy storage performance. Three levels of protection can be used to mitigate the propagation of thermal runaway: 1) Cell-to-cell; 2) Module-to-Module; 3) Pack level [12]. Whilst cell-to-cell is the most effective in containing thermal runaway, it is inaccessible for many electric vehicle manufacturers as modules are externally sourced. This has led to a major gap in literature on pack-level design. This paper aims to fill this gap by developing a battery pack enclosure that is tailor-made to reduce the severity of thermal runaway events. The proposed design of battery packs primarily focuses

This work was supported by the European Union’s Horizon 2020 research and innovation programme under the Marie Skłodowska-Curie Grant Agreement No. 872172 TESTBED2 project.

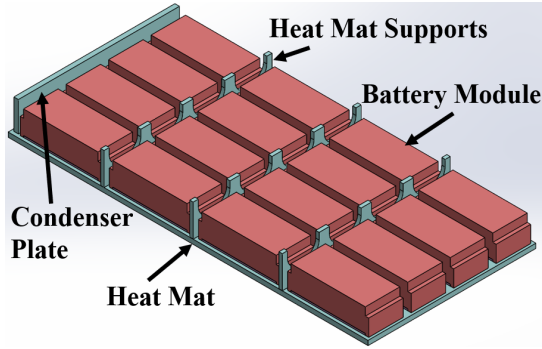


Fig. 1. Top: Labelled cooling plate cooling method; Bottom: Module and cooling plate assembly configuration.

on the prevention of thermal runaway propagation. Analyses of cells with insulation and without insulation are performed and comparison results are given. Additionally, thermal runaway simulations are used to develop understandings about the propagation of thermal runaway in a battery pack.

II. BATTERY PACK DESIGN AND ANALYSIS

This research is comprised of individual investigations that led to the comprehensive design and analysis of an electric vehicle battery pack suitable for use in the electrification of light-duty goods vehicles (LGVs) and heavy-duty goods vehicles (HGVs).

A. New Battery Pack Design

Although this battery pack deviated from industry front-runners in the primary focus of the design, there are core concepts that had to be incorporated to ensure the battery pack was representative of current technology. An industry-leading BYD T9 fully electric semitrailer has a capacity of 350 kWh [13]. Therefore, a feasible configuration of multiple battery packs must match this. To achieve this, CATL 14.8V 180Ah NMC battery modules were used. In one battery pack 32 of these modules were connected in series to provide a pack capacity of 82.25 kWh. With 4 packs, a vehicular capacity of 341 kWh meant the design was within current industry expectations. Figure 1 highlights the components of the pack such as the cooling plate and modules. Although the ancillary components were omitted from the design, adequate space was left in the design to ensure a realistic design.

A heat mat as the primary method of cooling accounts for the dissipation of 60% of the module's generated heat alone. The remaining 40% is dissipated naturally through convection and thermal radiation [14]. Additional characteristics include an even distribution of temperatures across all modules during normal operation, and the removal of high-energy-consuming coolant pumps. This investigation modelled the heat mat as a solid object on the assumption that temperatures experienced during thermal runaway rule the refrigerant ineffective. This assumption consequently reduces mesh complexity and scope for FEA computation errors. However, these assumptions

mean the technology analysed is more aptly described as a base cooling plate.

Methods of securing the packs to vehicles vary greatly due to differing spatial constraints and design criteria. However, a necessary design feature are compatible mounting points between the pack and the chassis. The enclosure frame was made using 25mm×25mm×4mm RSA structural members.

B. Thermal Runaway Analyses with/without Insulation

Once a design was established for the battery enclosure, thermal simulations were used to develop an understanding of the behaviour of a battery pack using a cooling plate under thermal runaway conditions. A thermal runaway event was modelled in Solidworks using the thermal simulation package for 2 iterations of 4 separate studies. The first iteration modelled a battery pack with no insulation and the second iteration included inter-module insulation and polymer supports. Figure 2 is an exploded view of the two iterations of testing with the supports omitted for clarity.

Figure 3 demonstrates the numbering convention of the modules that will be referred to throughout this report. Only modules 1, 4, 6, and 7 were chosen as the trigger modules due to the symmetry of the module. Furthermore, these modules represent the worst-case scenarios for trigger modules, with modules 6 and 7 both having 8 neighbours, and modules 1 and 4 being at the edges of the cooling plate. Data sensors were set to each component to track the average temperature over the duration of the study.

The simulation was a transient thermal study with a total study time of 300 s and a time increment of 2 s. This allowed adequate time for the thermal energy from the trigger module to propagate throughout the model and provide insight into likely propagation points in the design. This amount of time also captures the whole temperature profile of a module undergoing thermal runaway. Similarly, the temperature profile used for the trigger module was derived from the one obtained experimentally by Xu *et al.* in [15]. Figure 4 shows the temperature profile of the simulation overlaid with the profile from the reference [15]. All other parameters and material properties used for this study are outlined in Table I. All material property values were taken from the Solidworks materials library unless otherwise cited.

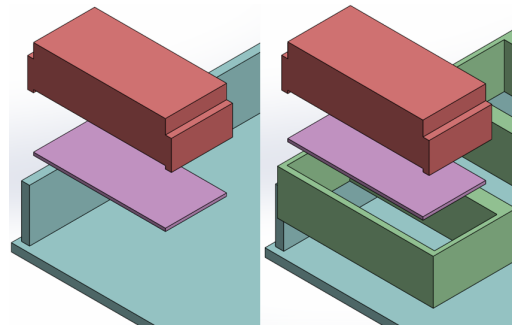


Fig. 2. Exploded view of the thermal simulation assembly with insulation (right) and without (left).

TABLE I
MATERIAL AND GLOBAL PARAMETERS USED IN THE THERMAL SIMULATIONS

Component	Parameter	Value	Unit
Global	Bulk Ambient Temperature	293	K
	Component Initial Temperature	293	K
	Surface convection coefficient	13.75	$W/(m^2.K)$
Module	Material	Cast Alloy Steel	-
	Thermal conductivity	38	$W/(m.K)$
	Specific heat	440	$J/(kg.K)$
Cooling plate	Material	Aluminium Alloy 1060	-
	Thermal conductivity	200	$W/(m.K)$
	Specific heat	900	$J/(kg.K)$
Support Brackets	Material	Aluminium Alloy 1060	-
	Thermal conductivity	200	$W/(m.K)$
	Specific heat	900	$J/(kg.K)$
Thermal Transfer Pad [16]	Material	THERM-A-GAP™ 579	-
	Thermal conductivity	3.0	$W/(m.K)$
	Specific heat	1000	$J/(kg.K)$
Thermal Insulation [17]	Material	Pyrogel® XTE	-
	Thermal conductivity	0.02	$W/(m.K)$
	Specific heat	1010	$J/(kg.K)$
Insulated Supports	Material	PPE	-
	Thermal conductivity	0.28	$W/(m.K)$
	Specific heat	1386	$J/(kg.K)$

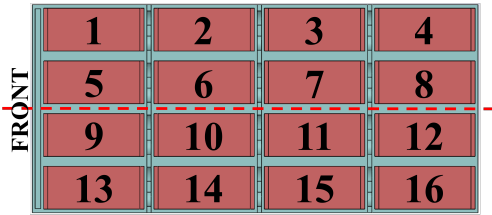


Fig. 3. Module numbering convention for thermal runaway simulations. The line of symmetry is also portrayed.

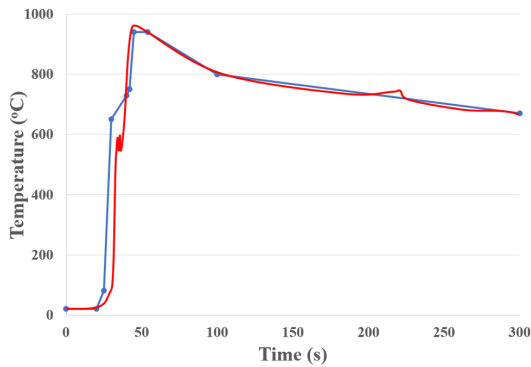


Fig. 4. Temperature profile of the trigger module (blue) and the temperature profile (red) of a module undergoing thermal runaway in [15].

Figure 4 shows modules undergoing thermal runaway will experience a rapid increase in temperature from normal operating temperatures of 298K (about 25°C) to nearly 1200K (about 927°C) in under 15 s. As the interval time in the simulation was 2 s, an exact likeness in profiles was not necessary as the simulation would not capture it. The disparity between the two profiles was within an acceptable tolerance as the most

important information to be captured was the amount of time at higher temperatures.

As this test is focused on propagation prevention and the most likely modules for the thermal runaway to propagate to initially are the neighbouring modules, the simulation domain only included one layer of cooling plate and modules. Equally, a full-pack thermal runaway event would be triggered if the energy released from the trigger module was great enough to trigger thermal runaway in a neighbouring module - this reaction would propagate. This assumption was validated with preliminary simulations of two layers of cooling plate and module assemblies that found that the greatest heat transfer into stable modules was into neighbouring modules of the same layer.

Bulk ambient temperature and component initial temperature were set at 293 K - a temperature typical of normal operating conditions. The components used in this simulation were assumed to be isothermal initially, as is typical in battery packs with base plate cooling systems after a sustained period of normal operation [14]. The surface convection coefficient was set at 13.75 W/m^2K as this represents free convection in air [18]. There is assumed to be no flow of air in the enclosure during operation as it would be sealed with no fan cooling method drawing air in. The homogeneity of the battery module material is the most substantial assumption. Battery modules are comprised of polymers and metals amongst many other materials but were modelled as cast alloy steel due its thermal properties. The module material needed to be effective in transferring the thermal energy to the cooling plate, yet the modules are also composed of polymers which have worse thermal transferring properties. To compromise, a metal with lower thermal transferring properties was selected. The selection of the module material did not have to be precise

in this regard, as conclusions drawn from overestimating the thermal capabilities consequently account for a greater safety factor in the results. Although consideration beyond safety requirements is not commercially viable, this research considered this factor immaterial. To improve thermal contact between the base of the module and the cooling plate, a sheet of THERM-A-GAP™ was sandwiched between the two.

III. RESULTS AND DISCUSSION

The thermal simulations provided insight into the behaviour of a base plate cooled battery pack in the event of thermal runaway. Transient average temperature data is presented in both Figure 5 and Figure 6.

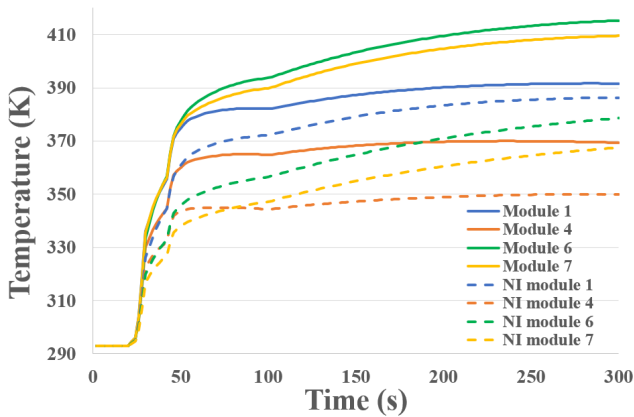


Fig. 5. Average temperature of the cooling plate in all simulations. “Module 1” refers to the test conducted with the trigger module in location 1 and insulation was added. The “NI” in the legend denotes the simulations where ‘no insulation’ was used.

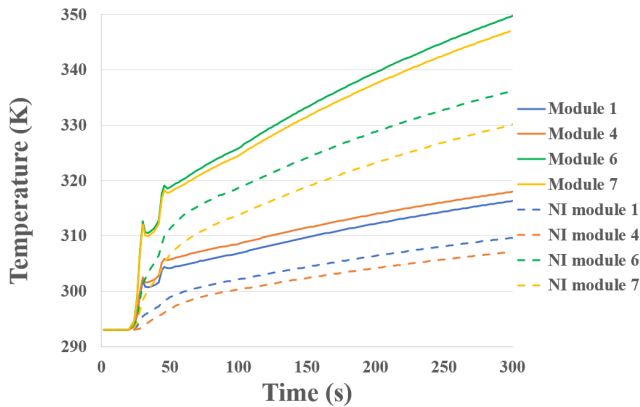


Fig. 6. Average temperature of the non-trigger modules.

The simulation with the greatest average cooling plate temperature without insulation was trigger location at module 1. This was due to its proximity to the condenser plate section of the cooling plate where large quantities of heat transfer occurred due to radiation and convection from the trigger module. The condenser plate acted as a heat sink in this simulation to such an extent that the average temperature consistently exceeded that of the locations enclosed by neighbouring modules. This was because the condenser plate was only 10 mm from the module whereas neighbouring

modules have a separation of 35 mm - facilitating greater heat transfer. Location 1 also had the smallest increase in average temperatures across both simulations. The added insulation worked both to limit thermal transfer to the condenser plate and extra thermal isolation.

On the other hand, location 6 produced both the highest average non-trigger module and cooling plate temperatures across all but one simulation. Locations 6 and 7 had similar responses with and without insulation, but location 6’s closer proximity to the condenser plate once again caused greater heat transfer to the cooling plate. The introduction of insulation reduced heat transfer through the condenser plate, as seen by the narrowing in the difference between the profiles of locations 6 and 7 across both tests.

All locations saw an increase in the average temperature of the cooling plate with the addition of thermal insulation. Although this was not intended, it provided a method of qualifying the impact of radiation and convection in the cooling of the modules. Insulation greatly inhibited the rejection of heat by radiation and convection across the whole model and as a result, the cooling plate retained heat more effectively, evidenced in Figure 5. A greater difference in average non-trigger module and cooling plate temperature was observed in locations 6 and 7 than in 1 and 4. Primarily due to the impact of the propagation through the insulation being magnified in locations 6 and 7 because of their central location. For locations 1 and 4, where modules are located at the extremities, thermal energy is more easily dispersed to the surrounding volume of air. Whereas in locations 6 and 7 this energy entered neighbouring modules.

In the event of thermal runaway, a large drawback of the base plate cooling method is its isothermal tendencies. During normal operation, this maintains a stable temperature across modules. However, during thermal runaway, it can act as a heat transfer agent for high temperatures to reach other modules. Figure 6 shows the response of the average temperature of all non-trigger modules in the simulation. Both with and without insulation the average temperature is increasing at a much more rapid pace than in the cooling plate. As the cooling plate has a higher average temperature, module temperatures continue to increase beyond the simulation period. Neighbouring modules gain thermal energy from either radiation, convection, conduction through the cooling plate, conduction through the thermal transfer pad, or conduction through the insulation. With the cooling plate having a thermal conductivity 100 times greater than comparable heat transfer modes, it was responsible for the main transfer of the thermal energy across the cooling plate.

As a result of insulation contact between modules and support, more heat was transferred via conduction in the insulated simulations. Therefore, there was a quicker, more widespread propagation of high temperatures with a larger epicentre. Figure 7 shows the behavioural differences in the dissipation of heat between both simulation models. Temperatures in these plots were taken from the top surface of the cooling plate for trigger module location 7 simulations. The

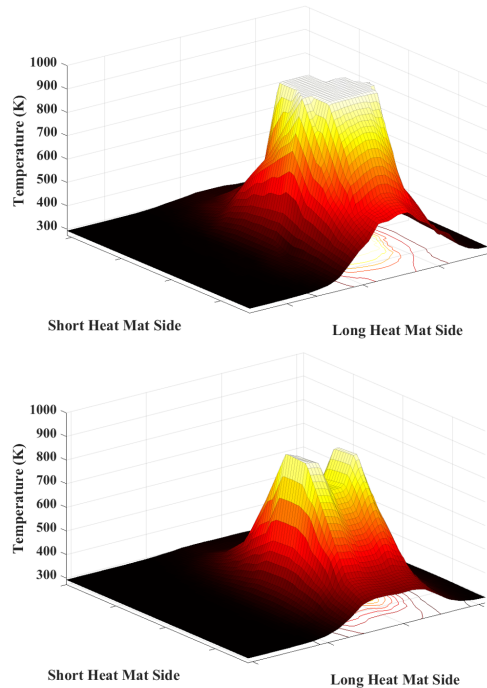


Fig. 7. Surfs of the cooling plate temperatures with trigger module 7 for the insulated battery pack (top) and non-insulated battery pack (bottom).

distinct two peaks in non-insulated conditions correspond to the points at which the module directly contacts the cooling plate without the thermal gap pad. This can be rationalised as the difference in thermal conductivity between the thermal gap pads and the module material. With the cooling plate being greater. However, these peaks reach a maximum of 64 K lower than the insulated conditions which also has a widespread peak. The widespread peaks were due to the ease at which conduction took place between the trigger module and the insulation at extremely high temperatures. Pyrogel XTE itself has varying thermal conductivity values dependent on its temperature. These results were obtained assuming a lower constant value. Despite this, the magnitude of the temperature gradient meant that the insulation also became a conduit for the thermal energy to propagate - an important conclusion for future design considerations.

Despite the insulation creating a worse heat-rejecting design, the direction of the heat transfer provides promise in future design developments. Figure 8 shows the root mean squared (RMS) of the resultant heat flux that passed through both the thermal gap pad below the trigger module and the faces of the trigger module that contacted the cooling plate directly. As these were the only entities contacting the cooling plate directly from the trigger module, these readings detail the resultant heat flux from the trigger module to the cooling plate through conduction only. The RMS was measured to remove the directional quantity of heat flux.

The clear disparity between the two simulations shows that even at its peak, the trigger module without insulation delivers over 1.5 times more energy directly to the cooling plate than if

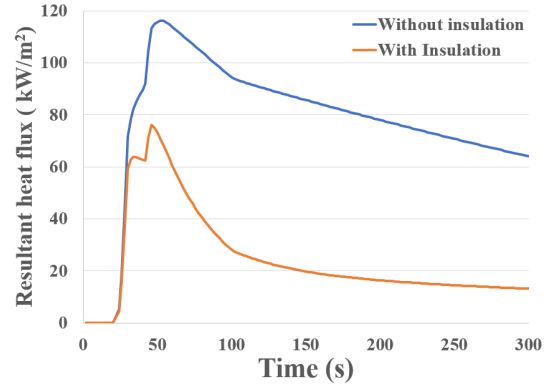


Fig. 8. Resultant heat flux passing through the thermal gap pad and module faces contacting the cooling plate.

the module was insulated. Thermal energy from the modules has an alternate route in the case of the insulated design. Although this propagates the high temperatures at a quicker rate, removal of energy from modules provides promising development opportunities for the possible integration of phase change materials (PCM) or a heat sink. These aim to transfer large amounts of energy from the locations most likely to propagate thermal runaway. Thermal energy travelling to both the cooling plate and insulation explains the sharper peak in heat flux with insulation at 50 s. At this stage, the temperature of the trigger module begins to cool and most of the module's conductive thermal rejection is going into the aluminium cooling plate as it is better at dispersing the energy across its entirety than other materials in the simulation. Equally, the cooling plate is a larger component than the insulation so will act as a better heat sink and maintains a steeper temperature gradient.

A limitation in the simulation which prevented a more comprehensive modelling of a full battery pack thermal runaway event was the inability to program a chain reaction. As previously mentioned, the critical temperature at which thermal runaway can be assumed is 100°C or 373 K. Figure 9 is an iso clipping of all locations in the battery pack above this critical temperature for trigger point 7. Thermal runaway would have propagated to modules within its boundaries and subsequently, the entire model.

Figure 9 further verifies the conclusion that the cooling plate acts as a channel for thermal transfer. In both test scenarios, the critical temperature is most widespread in the cooling plate itself and is then propagating upwards into the module. However, the insulation provides an extra channel for conductive heat transfer between modules resulting in a greater presence of above critical temperature conditions. Changing material of the supports to a thermally insulating material was extremely beneficial in preventing the propagation of high temperatures. As can be seen by the difference in the extent of the propagation of high temperatures in the supports across both models in Figure 9. It was not considered vital in this model for the supports to have the mechanical properties of a metal, especially because of the increase in the material properties

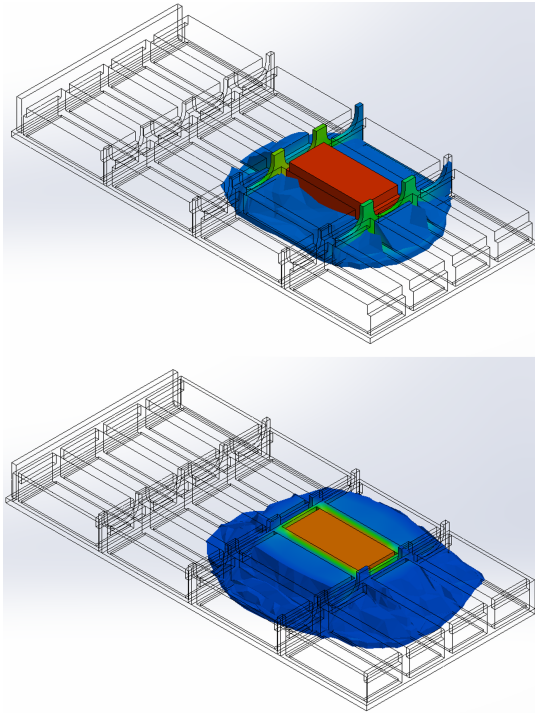


Fig. 9. Iso clipping at 100°C for non-insulated pack (top) and insulated pack (bottom).

of high-performing polymers. Further calculations into this may reveal this importance, but the improvement in thermal performance is so significant that a level of compromise must be considered.

The most prominent design feature causing the insulation to be detrimental was its direct contact with the module. It was modelled this way with consideration of the practical uses of this battery pack. Insulation close to the module after manufacture would come in direct contact with the modules after repeated movement of the vehicle during operation. However, different insulation materials and strategies not considered in this project could show more beneficial characteristics.

IV. CONCLUSIONS

This paper took a holistic approach to the characterisation of thermal runaway propagation at a pack level in electric truck applications. The battery pack consisted of two levels of cooling plates with 16 CATL 14.8V 180Ah NMC battery modules on each. Thermal interface material was added between the module and the cooling plate for better energy transfer. The work concluded that, because conduction is the main method of heat transfer, battery packs utilising a cooling plate cooling system will be inherently at greater risk of thermal runaway propagation. Thermally conductive materials are necessary for reliable performance during normal operation but are a major drawback during thermal runaway events. This research focused mainly on thermal simulations to characterise the behaviour of thermal runaway propagation and evaluate the success of propagation prevention mechanisms. Thermal insulation in direct contact with each of the modules was

ineffective in containing the high temperatures but reduced the maximum conductive load into the cooling plate from the trigger module by 33%. A direct extension of this research would be the evaluation of the effectiveness of phase change material or a heat sink at slowing the rate of propagation.

REFERENCES

- [1] M. Carlier and Statista. Battery electric vehicles in use - worldwide 2016-2020. (Accessed January 2022). [Online]. Available: <https://www.statista.com/statistics/270603/worldwide-number-of-hybrid-and-electric-vehicles-since-2009/>
- [2] U.K. Department of Transport. (Accessed January 2022). [Online]. Available: <https://www.gov.uk/government/news/government-takes-historic-step-towards-net-zero-with-end-of-sale-of-new-petrol-and-diesel-cars-by-2030>
- [3] X. Feng *et al.*, "Thermal runaway mechanisms of li-ion battery for electric vehicles: A review," *Energy Storage Materials*, vol. 10, pp. 246–267, 2018.
- [4] E. Sahraei *et al.*, "Characterizing and modeling mechanical properties and onset of short circuit for three types of lithium-ion pouch cells," *Journal of Power Sources*, vol. 247, pp. 503–516, 2014.
- [5] S. Wilke *et al.*, "Preventing thermal runaway propagation in lithium-ion battery packs using a phase change composite material: An experimental study," *Journal of Power Sources*, vol. 340, pp. 51–59, 2017.
- [6] W. Gao *et al.*, "Case study of an electric vehicle battery thermal runaway and online internal short-circuit detection," *IEEE Transactions on Power Electronics*, vol. 36, no. 3, pp. 2452–2455, 2021.
- [7] J. Jagemont *et al.*, "A comprehensive review of lithium-ion batteries used in hybrid and electric vehicles at cold temperatures," *Applied Energy*, pp. 99–114, 2016.
- [8] Elmelin Marketing. (Accessed April 2022). [Online]. Available: <https://elmelin.com/what-is-thermal-runaway-and-how-can-it-be-addressed/>
- [9] B. Xia *et al.*, "A correlation based fault detection method for short circuits in battery packs," *Journal of Power Sources*, vol. 337, pp. 1–10, 2016.
- [10] X. Feng *et al.*, "Online internal short circuit detection for a large format lithium ion battery," *Applied Energy*, vol. 161, pp. 168–180, 2016.
- [11] L. Shui *et al.*, "Design optimisation of battery pack enclosure for electric vehicles," *Structural and Multidisciplinary Optimization*, vol. 58, pp. 331–347, 2018.
- [12] J. Williamson, "Electric vehicle batteries: Managing thermal runaway vital to raising safety," 12 2018, (Accessed December 2021).
- [13] H. Liimatainen *et al.*, "The potential of electric trucks – an international commodity-level analysis," *Journal of Applied Energy*, vol. 236, pp. 804–814, 2019.
- [14] H. Jouhara *et al.*, "Investigation, development and experimental analyses of a heat pipe based battery thermal management system," *International Journal of Thermofluids*, p. 100004, 2020.
- [15] C. Xu *et al.*, "Experimental study on thermal runaway propagation of lithium-ion battery modules with different parallel-series hybrid connections," *Journal of Cleaner Production*, vol. 284, p. 124749, 2021.
- [16] Parker Hannifin Corp, *Thermal Interface Materials For Electronics Cooling Products & Custom Solutions Catalog*, Parker Chometrics, High Wycombe, UK, 2021.
- [17] Aspen Aerogels Inc, *Pyrogel-XTE-Datasheet*, Aspen Aerogels Inc, Massachusetts, USA, 2017.
- [18] P. Kosky *et al.*, *Exploring Engineering: An Introduction to Engineering and Design*, 5th ed. Academic Press, 2020.
- [19] K. Nice. (Accessed March 2022). [Online]. Available: <https://auto.howstuffworks.com/car-driving-safety/accidents-hazardous-conditions/crash-test.htm>